

KINESOFT: LEARNING PROPRIOCEPTIVE MANIPULATION POLICIES WITH SOFT ROBOT HANDS

Anonymous authors

Paper under double-blind review

ABSTRACT

Underactuated soft robot hands offer inherent safety and adaptability advantages over rigid systems, but developing dexterous manipulation skills remains challenging. While imitation learning shows promise for complex manipulation tasks, traditional approaches struggle with soft systems due to demonstration collection challenges and ineffective state representations. We present KineSoft, a framework enabling direct kinesthetic teaching of soft robotic hands by leveraging their natural compliance as a skill teaching advantage rather than only as a control challenge. KineSoft makes two key contributions: (1) an internal strain sensing array providing occlusion-free proprioceptive shape estimation, and (2) a shape-based imitation learning framework that uses proprioceptive feedback with a low-level shape-conditioned controller to ground diffusion-based policies. This enables human demonstrators to physically guide the robot while the system learns to associate proprioceptive patterns with successful manipulation strategies. We validate KineSoft through physical experiments, demonstrating superior shape estimation accuracy compared to baseline methods, precise shape-trajectory tracking, and higher task success rates compared to baseline imitation learning approaches. KineSoft’s results demonstrate that embracing the inherent properties of soft robots leads to intuitive and robust dexterous manipulation capabilities. Videos and code will be available upon final decision.

1 INTRODUCTION

Underactuated soft robotic hands offer significant advantages over rigid counterparts, including inherent safety through material compliance (Yoo et al., 2025) and robust adaptability to uncertain object geometries (Bhatt et al., 2022; Homberg et al., 2019; Yao et al., 2024). These properties make them particularly well-suited for applications requiring close human-robot interaction, such as assistive robotics, and collaborative manufacturing (Yoo et al., 2025; Firth et al., 2022). However, imparting dexterous in-hand manipulation skills to soft hands remains challenging. Traditional methods for soft robot manipulation often rely on hand-crafted primitives (Bhatt et al., 2022; Yao et al., 2024; Abondance et al., 2020) that necessitate expert operators and limit system adaptability.

Recent advances in imitation learning, particularly frameworks like diffusion policy, have shown promise in teaching complex manipulation skills (Chi et al., 2023; Memmel et al., 2025; Hu et al., 2023). These approaches have been successfully applied to various tasks, from long-horizon mobile manipulation with rigid grippers (Fu et al., 2024) to deformable object manipulation with simple end-effectors (Yoo et al., 2024a). Unlike reinforcement learning methods that depend on carefully crafted reward functions and simulation environments (Qi et al., 2025; Wang et al., 2024), imitation learning requires only demonstration trajectories of successful task execution. However, collecting such demonstrations for soft hands presents challenges: traditional demonstration collection methods generally do not apply to underactuated soft systems with virtually infinite degrees of freedom. Conventional teleoperation interfaces (Qin et al., 2023), designed for rigid anthropomorphic hands, fail to capture the unique capabilities and constraints of underactuated soft end-effectors, which often lack an intuitive mapping to rigid human hand joints. Additionally, standard robot state representations for rigid robots in imitation learning frameworks (Ze et al., 2024), such as rigid transformation poses, struggle to provide meaningful state information when applied to continuously deforming structures. Despite recent advancements in expressive state representation learning for soft robots (Wang et al., 2023; Yoo et al., 2023; 2024b), these have not yet been applied to skill

054
055
056
057
058
059
060
061
062
063
064
065
066
067
068
069
070
071
072
073
074
075
076
077
078
079
080
081
082
083
084
085
086
087
088
089
090
091
092
093
094
095
096
097
098
099
100
101
102
103
104
105
106
107

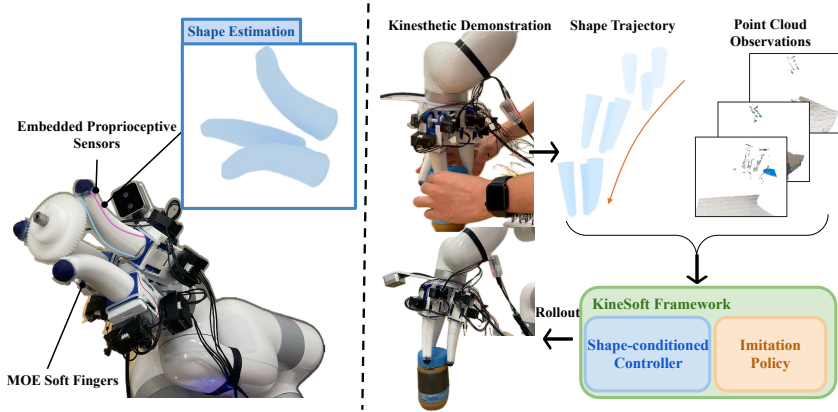


Figure 1: **KineSoft** is a framework for learning from kinesthetic demonstration, enabling free-shaped soft end-effectors to perform dexterous in-hand manipulation. Three key components are: 1) proprioceptive model for high-fidelity shape estimation, 2) diffusion-based imitation learning for predicting the changes in shape and end-effector poses, and 3) shape-conditioned controller that allows the soft hand to track given shape trajectories.

learning frameworks for in-hand manipulation. These limitations have restricted the application of imitation learning to soft robotic manipulation.

We present KineSoft, a hierarchical framework that enables direct kinesthetic teaching of soft robotic hands. Our key insight is that soft robots’ natural compliance is an advantage for teaching rather than just a control challenge. This compliance allows human demonstrators to physically guide the soft robot fingers through desired movements, enabling intuitive demonstration collection that naturally accounts for the system’s mechanical properties without fighting against kinematic constraints. As shown in Figure 1, KineSoft is composed of three key components. First, the proprioceptive system achieves state-of-the-art shape estimation using internal strain sensing arrays and a model trained on large simulated data of the robot’s high-dimensional configurations. These sensors provide rich proprioceptive feedback while preserving the hand’s natural compliance, allowing KineSoft to capture detailed information about the hand’s deformation state during manipulation tasks in real time. Next, we train an imitation policy on these shape trajectories and use it to generate deformation trajectories during rollout. Finally, KineSoft’s low-level shape-conditioned controller then tracks these desired shapes. Experiments demonstrate that KineSoft achieves accurate shape state estimation, precise trajectory tracking through the shape-conditioned controller, and superior performance in learned manipulation tasks through these shape-based representations.

In summary, this paper provides the following contributions: **i)** KineSoft, a framework for learning from kinesthetic demonstrations for soft robot hands that enables dexterous in-hand manipulation, **ii)** a state-of-the-art proprioceptive shape estimation approach using strain sensing integrated with soft robot hands that enables precise tracking of finger deformations during contact-rich tasks, **iii)** shape-conditioned controller for tracking the generated deformation trajectories and performing dexterous manipulation tasks, and **iv)** simulated dataset and trained model for state estimation and control, which we demonstrate can be readily deployed to open-source soft robot hands, such as the MOE platform (Yoo et al., 2025).

2 RELATED WORK

Learning for in-hand dexterity. Recent advances in reinforcement learning have driven significant progress in rigid robot in-hand dexterity (Wang et al., 2024; Qi et al., 2025; Yao et al., 2024; Andrychowicz et al., 2020). However, these approaches face challenges in real-world deployment due to difficulty in creating resettable training environments. To mitigate these issues, many methods transfer policies trained in simulation to the real world, which has shown success with rigid robots with fine tuning in the real world (Qi et al., 2025; Wang et al., 2024) but remains less applicable for soft robots due to the complexities involved in modeling deformable materials, forward

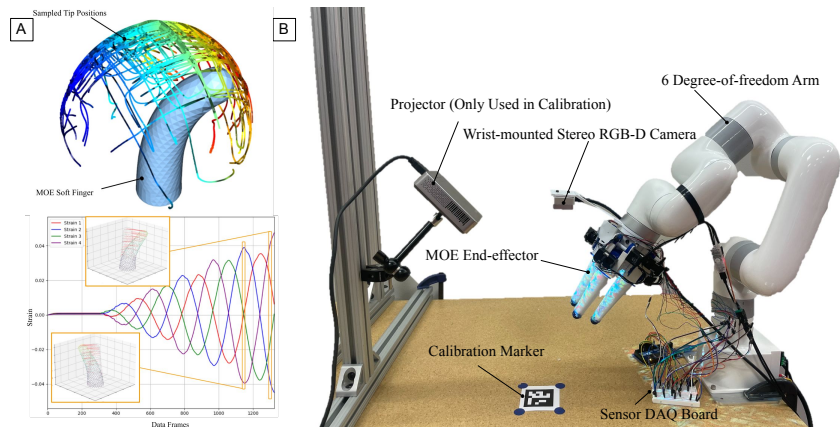


Figure 2: **Simulated and real-world setup.** A: Simulated robot workspace and sample of simulated strain signals. B: Real-world robot setup with the projected patterns to improve ground-truth shape observations for evaluation and calibration.

kinematics, and contact dynamics (Della Santina et al., 2023). Despite recent interest in leveraging reinforcement learning for soft robot arm control and trajectory tracking (Thuruthel et al., 2018; Schegg et al., 2023; Bhagat et al., 2019), difficulty in modeling simultaneous contact and soft robot body deformation dynamics have hindered their application to soft robot dexterous manipulation.

Imitation learning has emerged as a promising alternative for reducing the reliance on explicit physics simulation environments, enabling robots to acquire manipulation skills efficiently with real-world data (Johns, 2021; Chi et al., 2023; Ze et al., 2024). In-hand manipulation skills through imitation learning are typically achievable with anthropomorphic hands that provide an intuitive mapping between human hand and robot poses (Arunachalam et al., 2023a;b; Wei & Xu, 2024). However, despite inherent benefits in safety and dexterity through compliance, which soft robot hands naturally provide, soft robots were subject to some unique challenges—particularly due to the absence of reliable proprioceptive feedback (Weinberg et al., 2024) and thus the lack of practical frameworks for collecting demonstrations for soft robots. To the best of our knowledge, *KineSoft* is the first framework that effectively leverages passive compliance of the soft robots to collect demonstrations and enables soft robots to acquire dexterous in-hand manipulation skills.

Soft robot dexterity. Soft robot hands excel in grasping and manipulation tasks due to their material compliance, which allows passive adaptation to diverse object geometries (Rus & Tolley, 2015; Zhou et al., 2023). This compliance facilitates robust grasping and safe interactions with humans and delicate objects by distributing contact forces across large areas (Abondance et al., 2020; Liu et al., 2024; Yoo et al., 2025). Recent advancements in soft robotics have aimed to enhance dexterity through innovative actuator designs, material improvements, and bio-inspired morphologies (Puhlmann et al., 2022; Firth et al., 2022). Despite these strides, controlling soft hands remains a significant challenge due to their complex dynamics and the high-dimensional nature of their deformation spaces (Yasa et al., 2023). Consequently, learning-based approaches for soft robotic dexterity have primarily focused on grasping (Gupta et al., 2016), while the development of dexterous in-hand manipulation skills has been hindered by the lack of intuitive demonstration methods and reliable proprioceptive feedback (Weinberg et al., 2024). The unique advantages of soft robot hands in robust in-hand manipulation stem from their lack of rigid skeletal structures (Pagoli et al., 2021). However, this absence also introduces challenges, as soft robot kinematics differ significantly from human hand motions. The *KineSoft* framework bridges these gaps by integrating novel and accurate shape estimation methods with learned imitation policies, enabling efficient skill acquisition for dexterous manipulation with soft robots.

Soft robot state representation. Proprioceptive shape sensing is critical for enabling dexterous control in soft robots, particularly for accurate shape tracking and feedback-driven control (Zhou et al., 2024). Existing works often utilize low degree-of-freedom shape representations such as constant curvature models (Stella et al., 2023; Yoo et al., 2021) or bending angles (Wall et al., 2017), which fail to capture the full richness of soft robot deformation states. Toward capturing these complex de-

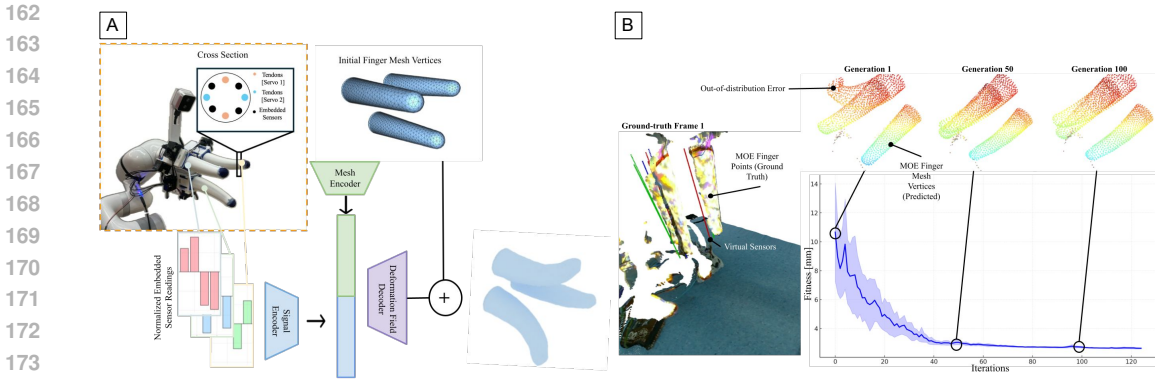


Figure 3: **Proprioception network.** A: Network architecture for mesh shape estimation of the soft fingers. B: Results of domain alignment iterations where the loss converged after 200 iterations.

formation behaviors of soft robot manipulators, recent approaches based on mechanics models have employed Cosserat rod models and high-dimensional Frenet–Serret frames, associated with the continuum cross sections (Liu et al., 2021). However, these approaches are computationally costly to update and to preserve hard constraints (Liu et al., 2021; 2020). Recent learning-based models have introduced more expressive representations of soft robot states using point clouds (Wang et al., 2023; Yoo et al., 2023) and meshes (Yoo et al., 2024b; Tapia et al., 2020). However, these learned representations have not been connected to policy learning for dexterous manipulation tasks. Addressing this gap, *KineSoft* proposes a novel framework that leverages proprioceptive sensing and learned shape representations, based on vertex displacement fields over meshes, to facilitate dexterous in-hand manipulation skill learning in soft robots.

3 PROBLEM STATEMENT

We consider the problem of dexterous in-hand manipulation with a soft robotic hand. Let \mathbf{M} represent the true underlying continuous deformation state space of the hand. The hand is actuated through a set of control inputs \mathbf{U} , with the relationship between actuation and deformation being governed by the hand’s material properties and mechanical design. The problem of learning dexterous manipulation skills consists of key challenges: i) we need an observable surrogate \mathbf{S} of the true deformation state space, ii) we need a reliable mapping between the surrogate space \mathbf{S} and the true deformation state space \mathbf{M} , and iii) we need a policy π , which maps the current state to appropriate control actions: $\pi : \mathbf{M} \times \mathcal{O} \mapsto \mathbf{U}$, where \mathcal{O} represents additional task-relevant observations. This presents unique challenges for soft robots compared to rigid systems: the continuous deformation space \mathbf{M} is theoretically infinite-dimensional as a continuum, demonstrations must account for the robot’s inherent compliance, and the mapping between actuation and deformation is highly nonlinear or difficult to simulate in its entirety (Liu et al., 2021). The objective is to develop a framework that can effectively learn and execute manipulation skills while embracing these fundamental characteristics of soft robots.

4 METHOD

4.1 MOE SOFT ROBOT END-EFFECTOR

In this work, we leverage the MOE soft robot platform, introduced by yoo2025soft, which comprises modular finger units that each operate independently. Each finger is actuated by two servo motors, which apply tension to four tendons, as shown in Figure 3. This modular design provides flexibility, allowing the fingers to be rearranged into various configurations to suit specific task requirements. In this study, we examine a three-finger variant of MOE, inspired by research on object controllability using three-fingered rigid end-effectors (Mason & Salisbury Jr, 1985).

Building on the original MOE finger design, we present an enhancement by embedding low-cost conductive elastic rubber directly into the silicone elastomer body of each finger. These sensors measure deformation by varying their electrical resistance as they stretch, providing real-time proprioceptive feedback. Each finger incorporates four of these sensors, compactly positioned between the tendons. The sensors are connected to a data acquisition (DAQ) circuit and board capable of recording resistance readings at approximately 400 Hz. By seamlessly integrating the sensors into the elastomer during fabrication, we developed a fully deformable and sensorized finger body. The combined state spaces from all twelve (12) strain sensors provides our estimate \mathbf{S} of the soft robot hand’s true deformation state space \mathbf{M} (Section 3).

In contrast to prior works (Tapia et al., 2020; Pannen et al., 2022), which relied on custom sensor fabrication or specialized materials, our proposed modifications to the MOE design leverage off-the-shelf conductive rubber, eliminating the need for complex manufacturing processes, enabling straightforward integration into robotic systems, and enhancing accessibility and scalability across a wide range of applications. Furthermore, we present a shape estimation model trained on large simulated soft robot dataset, which can be deployed on sensorized MOE hands through autonomous domain alignment as discussed in later sections.

4.2 SHAPE ESTIMATION MODEL

The objective of the shape estimation model is to learn a mapping between sensor readings from embedded strain sensors \mathbf{S} and the vertex displacements of the MOE fingers. Each finger contains four strain sensors arranged between the tendons, giving us $n = 12$ resistance measurements total for the three-fingered hand, denoted as $\mathbf{R} \in \mathbb{R}^n$.

The model learns a function f that maps from sensor resistance readings and initial vertex positions to displacement vectors. Let $\mathbf{V}_{j,0} \in \mathbb{R}^{N \times 3}$ denote the initial vertex positions of finger j , where N is the number of vertices in the mesh. The mapping can be expressed as:

$$f : (\mathbf{R}, \{\mathbf{V}_{j,0}\}_{j=1}^3) \mapsto \{\Delta\mathbf{V}_j\}_{j=1}^3$$

We implement this mapping using a FoldingNet-inspired architecture. The network first encodes each finger’s four strain measurements into a latent representation $\mathbf{z}_j \in \mathbb{R}^{128}$ through an encoding function:

$$\mathbf{z}_j = h_{\text{enc}}(\mathbf{R}_j)$$

The decoder then processes each vertex independently by learning a mapping from the concatenated initial vertex position and latent displacement:

$$\Delta\mathbf{v}_{j,i} = h_{\text{dec}}(\mathbf{v}_{j,0}^i, \mathbf{z}_j),$$

where $\mathbf{v}_{j,0}^i \in \mathbb{R}^3$ is the initial position of vertex i in finger j , and $[\cdot]$ denotes concatenation. This vertex-wise processing allows the network to learn local deformation patterns while maintaining spatial relationships defined by the initial mesh topology. The deformed vertex positions are then obtained by applying the predicted displacements:

$$\mathbf{v}_{j,t}^i = \mathbf{v}_{j,0}^i + \Delta\mathbf{v}_{j,i}$$

The FoldingNet decoder architecture enables learning vertex-level deformations while leveraging the spatial structure of the initial mesh configuration. By predicting displacements rather than absolute positions, the network learns naturally centered and scaled deformations, leading to more stable training and better generalization. To train the model, we generate a large dataset of deformed meshes using SOFA (Simulation Open Framework Architecture) (Westwood et al., 2007). Our simulation setup uses a tetrahedral finite element mesh of the MOE finger with a Neo-Hookean hyperelastic material model parameterized by elastic material properties that are randomized at runtime.

We model the tendon actuation with massless, inextensible cables running through a series of fixed points within the finger body. Each tendon path is discretized into segments defined by 3D attachment points embedded in the tetrahedral mesh. The cable constraint applies forces to these points to maintain constant length while allowing sliding, effectively simulating the mechanical behavior of Bowden cable transmission. The soft body scene is solved with an implicit Euler time integration scheme and uses a conjugate gradient solver for the system matrices. We generate training data by

randomly sampling tendon actuation commands within the feasible range and recording the resulting deformed vertex positions and embedded sensor strains. To simulate rich deformation behaviors including contact-like effects, we apply random external forces to the finger surface. These forces are randomly applied over time with sufficiently large radii to ensure smooth deformations that mimic natural contact interactions, without requiring explicit and difficult-to-model contacts in the scene.

The model is trained using mean squared error (MSE) loss on vertex displacements:

$$\mathcal{L} = \frac{1}{3N} \sum_{j=1}^3 \sum_{i=1}^N \|\Delta \mathbf{v}_{j,i} - \Delta \mathbf{v}_{j,i}^*\|^2,$$

where $\Delta \mathbf{v}_{j,i}^*$ represents the ground truth displacement for vertex i of mesh finger j . This choice of loss function provides strong supervision by enforcing explicit vertex-wise correspondence between predicted and ground truth meshes. Because we leverage simulated data to train the model, we can exploit the vertex-level correspondences in the meshes unlike prior works that had to rely on chamfer distance loss over real-world partial observations (Wang et al., 2020), MSE loss ensures that each vertex learns to track its specific local deformation patterns, enabling precise reconstruction of the full finger shape.

4.3 SIM-TO-REAL DOMAIN ALIGNMENT

We assume the embedded sensors are perfectly incompressible and isotropic, a common assumption in soft body mechanics for highly elastic rubber, particularly when infused with particle fillers (Starkova & Aniskevich, 2010). These fillers, like those used in the off-the-shelf conductive rubbers embedded in MOE, enable the sensors to exhibit changes in resistivity when stretched. The sensors have a cylindrical shape, so we model the relationship between the cross-sectional area and the strain in the axial direction for sensor i at time $t \geq 0$ with the incompressibility assumption as:

$$L_{i,0} A_{i,0} = L_{i,t} A_{i,t}, \quad (1)$$

where $L_{i,0}$ and $A_{i,0}$ are the initial length and cross-sectional area; $L_{i,t}$ and $A_{i,t}$ are the corresponding values at time t .

For conductive materials, resistance generally has a linear relationship with strain. The observed resistance for the sensor indexed at i is given by:

$$R_{i,t} = \rho_i \frac{L_{i,t}}{A_{i,t}}, \quad (2)$$

where ρ_i is the conductivity factor, assumed to be constant for sensor i across time. Relating Equation 1 and Equation 2, we derive:

$$\sqrt{\frac{R_{i,t}}{R_{i,0}}} - 1 = \frac{L_{i,t} - L_{i,0}}{L_{i,0}}. \quad (3)$$

This relationship is independent of the material conductivity ρ_i , enabling a direct mapping from observed resistance to strain. However, in real-world applications, fabrication imperfections, such as connecting wires to the DAQ boards, can introduce errors into the initial length of the embedded sensors. These imperfections result in a deviation between the real sensor lengths ($L_{i,0}^R, L_{i,t}^R$) and simulated sensor lengths ($L_{i,0}^S, L_{i,t}^S$):

$$L_{i,0}^R = L_{i,0}^S + \epsilon_i, \quad L_{i,t}^R = L_{i,t}^S + \epsilon_i,$$

where ϵ_i is a constant error specific to each sensor i . This error propagates to the strain relationship as:

$$\frac{L_{i,t}^R - L_{i,0}^R}{L_{i,0}^R} = \frac{1}{1 + \frac{\epsilon_i}{L_{i,0}^S}} \cdot \frac{L_{i,t}^S - L_{i,0}^S}{L_{i,0}^S} \quad (4)$$

The constant factor $\frac{1}{1 + \frac{\epsilon_i}{L_{i,0}^S}}$ can be denoted as $\kappa_i \in \kappa$, representing the constant correction factor for sensor i . Substituting this into Equation 3, we obtain:

$$\sqrt{\frac{R_{i,t}}{R_{i,0}}} - 1 = \kappa_i \frac{L_{i,t}^S - L_{i,0}^S}{L_{i,0}^S}, \quad (5)$$

where the observed resistances $R_{i,t}, R_{i,0}$ are measured with the DAQ setup. For the n embedded sensors, aligning the simulated and observed distributions involves optimizing the constant correction parameters $\kappa_0, \kappa_1, \dots, \kappa_{n-1}$. The objective is defined as:

$$\arg \min_{\kappa_0, \dots, \kappa_{n-1}} \sum_{i=0}^{n-1} \sum_{t=0}^{T-1} \left(\sqrt{\frac{R_{i,t}}{R_{i,0}}} - \kappa_i \frac{L_{i,t}^S - L_{i,0}^S}{L_{i,0}^S} - 1 \right)^2, \quad (6)$$

where T is the number of time steps for which resistance data is observed.

Finally, because the corresponding simulated lengths for an observed resistance are not available (i.e., there is no direct sim-to-real correspondence between the observed resistance values and the simulated lengths), we instead optimize the correction factors $\kappa_0, \kappa_1, \dots, \kappa_{n-1}$ by minimizing the Chamfer distance between the observed points on the fingers and the model’s predicted surface points. This optimization assumes that there is a unique mapping between the internal strain of the sensors and the deformation of the soft structure, which is inferred through the observed resistance values.

The model defines a mapping from the sensor resistance observations to the surface mesh of the fingers based on the predicted displacements of the vertices. However, in the real-world deployment of the model as shown in the Figure 2, we do not have access to labeled pairs of real-world resistance values \mathbf{R} and $\mathbf{L}^{\mathbf{R}}$:

$$\mathcal{L}_{\text{UCD}} = \sum_{j=0}^{m-1} \sum_{\mathbf{p}_{\text{obs}} \in \mathcal{P}_{\text{obs}}} \min_{\mathbf{v} \in \mathbf{V}_{j,t}} \|\mathbf{p}_{\text{obs}} - \mathbf{v}\|^2, \quad (7)$$

where \mathcal{P}_{obs} is the set of observed points on the surface of the fingers from the RGB-D camera feed and $\mathbf{V}_{j,t}$ are vertices of the predicted surface mesh of finger j defined by $\mathbf{M}_{j,t} = f(\mathbf{R}, \mathbf{V}_{j,0})$. We compute $\mathcal{L}_{\text{UCD}}(\kappa)$ where the correction factors κ_i are adjusted such that the predicted surface points align with the observed deformation of the fingers.

The function f is differentiable and thus gradient descent-based optimization is possible here for locally optimal κ . However, because of the noisy loss landscape and relatively cheap inference cost, we achieved better performance by optimizing κ with a sample-based evolutionary strategy (Hansen et al., 2003). By optimizing for the alignment factors κ , the model effectively aligns the observed resistance-to-strain relationship with the real-world deformation states, ensuring robust sim-to-real transfer for the shape estimation model.

4.4 SHAPE-CONDITIONED CONTROLLER

The shape-conditioned controller leverages real-time proprioceptive mesh state estimation of the MOE fingers to track desired shape trajectories. For each finger j , the controller compares the current estimated vertex positions \mathbf{V}_t with desired target positions \mathbf{V}_t^D generated from the policy trajectory. The shape residual is calculated over the corresponding vertices of the meshes:

$$\mathbf{e}_{j,t} = \mathbf{V}_{t,j}^D - \mathbf{V}_{t,j}$$

Each finger is actuated by a pair of antagonistic tendons controlled by two servos. The actuation directions for each servo pair are represented by unit vectors $\mathbf{d}_{2j}, \mathbf{d}_{2j+1} \in \mathbb{R}^2$ that capture the primary deformation modes. The servo adjustments $\delta u_{j,t}$ for each finger are computed by projecting the shape error onto these actuation directions:

$$\delta u_{j,t} = k_p \sum_n \mathbf{e}_{j,t}^n \cdot [\mathbf{d}_{2j}, \mathbf{d}_{2j+1}]^T$$

where k_p is a scalar gain and $\mathbf{e}_{j,t}^n$ is the error for vertex n . In deployment, the actions are clipped to prevent overloading the actuators. This controller runs at 100Hz with the shape estimation at each step, enabling responsive shape trajectory tracking. By projecting shape errors onto fitted actuation directions, the controller effectively translates desired deformations into appropriate servo commands despite the complex relationship between tendon actuation and finger deformation.

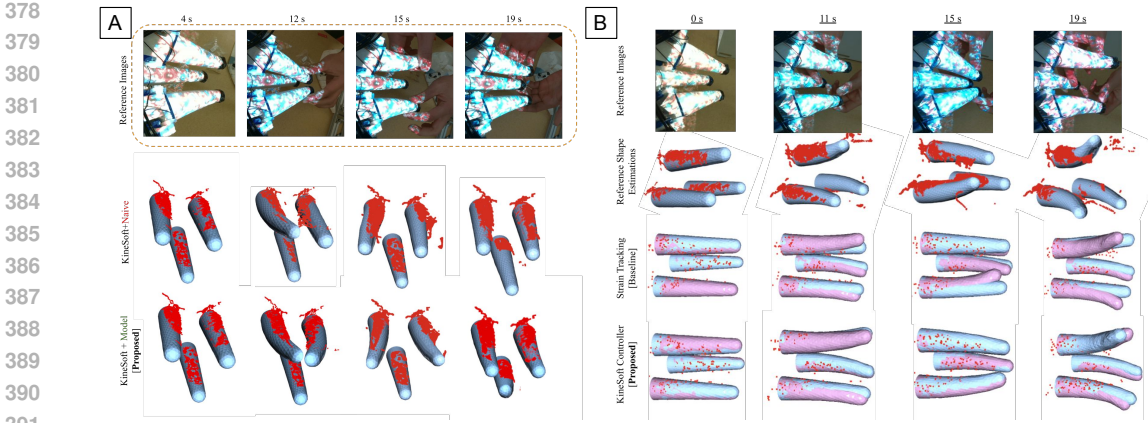


Figure 4: **Shape estimation and trajectory tracking performance evaluation.** We provide each of the shape estimation models and controllers with kinesthetically deformed shape trajectories. A: Shape estimation model comparisons with real-world ground-truth data (red points). B: Shape tracking comparisons with the real-world ground-truth data (red points), references shapes (red), and achieved shapes (blue).

4.5 IMITATION POLICY

The shape estimation model from Section 4.2 provides proprioceptive feedback through predicted vertex positions \mathbf{V}_t . The wrist-mounted RGB-D camera captures point cloud observations of the manipulation workspace. Using these complementary sources of state information, we train a diffusion policy to learn manipulation skills via imitation learning.

The policy predicts actions that combine shape deformations and end-effector pose changes:

$$a_t = \{\Delta \mathbf{V}_t, \Delta \mathbf{p}_t\}$$

The state representation combines two different point-based encodings:

$$s_t = \{h_{\text{shape}}(\mathbf{V}_t), h_{\text{pc}}(\mathcal{P}_t), \mathbf{p}_t\},$$

where h_{shape} processes the predicted vertex positions using MLPs that leverage vertex correspondence, h_{pc} is a DP3 point cloud encoder that processes subsampled RGB-D observations \mathcal{P}_t , and \mathbf{p}_t is the current end-effector pose.

The diffusion model iteratively denoises a Gaussian distribution into meaningful actions through a reverse process:

$$a_{t-1} = \mu_{\theta}(a_t, s_t, t) + \sigma_t \mathbf{z},$$

where μ_{θ} is a learned denoising model and $\mathbf{z} \sim \mathcal{N}(0, \mathbf{I})$.

The trained policy works with the shape-conditioned controller from Section 4.4, which maps the policy’s deformation predictions to actuator commands. This hierarchical approach enables robust manipulation by combining learned high-level behaviors with precise low-level tracking.

5 EXPERIMENTS

5.1 SHAPE ESTIMATION FIDELITY

We evaluated the proposed shape estimation model against two baseline methods from the literature: constant curvature model (Della Santina et al., 2020; Yoo et al., 2021), a common analytical approach for soft robot shape representation, and DeepSoRo (Wang et al., 2020), a learning-based point cloud reconstruction method. Additionally, we demonstrate that our soft body mechanics-based mapping between observed resistance values and simulated strains, as outlined in Section 4.2, substantially improves upon a naively calibrated linear mapping while using the same domain alignment approach proposed in Section 4.3.

Figure 3 visualizes this performance difference. While both controllers receive reference trajectories collected through kinesthetic teaching, the shape-conditioned controller successfully reproduces the demonstrated shapes using tendon actuation, even though the sensor signals during execution differ from those during the demonstration. The strain-tracking baseline exhibits larger errors because it attempts to match sensor readings that are different between demonstration and execution modes.

The improved shape tracking performance of KineSoft’s shape-conditioned controller stems from its ability to abstract away the differences in how deformations are achieved (manual guidance vs. tendon actuation) by focusing on the resulting geometric configurations. This shape-based abstraction provides a consistent representation across demonstration and execution, enabling functionally successful reproduction of demonstrated skills.

5.3 IN-HAND MANIPULATION TASK PERFORMANCE

We evaluated KineSoft on in-hand manipulation tasks requiring precise finger control and in-hand dexterity:

Cap Unscrewing: MOE makes contact with a bottle cap that is screwed on. Then it must coordinate the three fingers to rotate the cap sufficiently to unscrew it then raise it up. The task is considered successful if the initially screwed on container is detached from the bottle.

Container Unlidding: MOE initially grasps an empty container that has a closed hinged snap top lid. It must then lift up the container then move the fingers to the right positions and flip the lid open. To apply sufficient force on the lid, two of the MOE fingers must hold the container’s body while one of the fingers pries open the lid. The task is considered successful if the container lid is open in MOE’s grasp.

For each task, we collected 50 successful demonstrations through kinesthetic teaching, where an expert demonstrator physically guided the fingers through the required motions. This kinesthetic teaching approach highlights a key advantage of our framework: while humans can intuitively demonstrate complex manipulations by directly deforming the soft fingers, these demonstrated configurations must ultimately be achieved through tendon actuation during autonomous execution. This creates a gap, as the sensor signals during human demonstration (direct finger deformation) differ substantially from those during autonomous execution (tendon actuation). KineSoft bridges this gap by focusing on reproducing the demonstrated shapes rather than matching the sensor signals directly.

As shown in Table 3, KineSoft achieved a 100% success rate (5/5 trials) on the unscrewing task compared to 0/5 for the strain-matching baseline. The baseline policy failed primarily because it attempted to reproduce sensor signals from demonstration that were either impossible to achieve through tendon actuation alone or not grounded to the functionally correct robot states to perform the task. In contrast, KineSoft’s shape-based approach successfully translated the demonstrated trajectories into executable tendon commands that produced the desired finger configurations.

These results demonstrate that by focusing on tracking demonstrated shapes rather than raw sensor signals, KineSoft effectively bridges the gap between human demonstration and autonomous execution. The shape estimation model provides a consistent representation across both modes, while the shape-conditioned controller reliably reproduces the demonstrated behaviors despite the gap in how deformations are achieved.

Method	Representation	Error (mm)
Strain-tracking	Strain	6.20 ± 2.39
KineSoft	Mesh	3.29 ± 0.91

Table 2: Shape Tracking Error Comparison

Task	Policy	Success Rate
Cap Unscrewing	Strain-Matching	0/5
	KineSoft	5/5
Container Unlidding	Strain-Matching	0/5
	KineSoft	4/5

Table 3: Task Performance Across Different Policies

6 CONCLUSION AND LESSONS

This paper presents KineSoft, a framework for learning dexterous manipulation skills with soft robot hands that embraces, rather than fights against, their inherent compliance. The key insight of our work is recognizing that while this compliance enables intuitive kinesthetic teaching, it creates a fundamental gap between demonstration and execution, where the deformations and sensor signals during human demonstration differ substantially from those during autonomous execution through tendon actuation.

KineSoft addresses this challenge through a hierarchical approach. A shape estimation model provides consistent geometric representations across demonstration and execution modes while a domain alignment method enables robust transfer of simulation-trained models to real hardware and a shape-conditioned controller reliably tracks the policy’s generated deformation trajectories despite the different underlying actuation mechanisms. Then, a high-level imitation policy learns to generate target vertex deformations from demonstrations, capturing the intended manipulation strategy in geometric grounding. Our experimental results demonstrate that this shape-based hierarchical approach enables more effective skill transfer than methods that attempt to directly match sensor signals or joint configurations. This work suggests that successful imitation learning for dexterous soft robots requires careful consideration of how demonstration and execution modes differ, and appropriate intermediate representations to bridge this gap.

REFERENCES

- Sylvain Abondance, Clark B Teeple, and Robert J Wood. A dexterous soft robotic hand for delicate in-hand manipulation. *IEEE Robotics and Automation Letters*, 5(4):5502–5509, 2020.
- OpenAI: Marcin Andrychowicz, Bowen Baker, Maciek Chociej, Rafal Jozefowicz, Bob McGrew, Jakub Pachocki, Arthur Petron, Matthias Plappert, Glenn Powell, Alex Ray, et al. Learning dexterous in-hand manipulation. *The International Journal of Robotics Research*, 39(1):3–20, 2020.
- Sridhar Pandian Arunachalam, Irmak Güzey, Soumith Chintala, and Lerrel Pinto. Holo-dex: Teaching dexterity with immersive mixed reality. In *2023 IEEE International Conference on Robotics and Automation (ICRA)*, pp. 5962–5969. IEEE, 2023a.
- Sridhar Pandian Arunachalam, Sneha Silwal, Ben Evans, and Lerrel Pinto. Dexterous imitation made easy: A learning-based framework for efficient dexterous manipulation. In *2023 IEEE international conference on robotics and automation (icra)*, pp. 5954–5961. IEEE, 2023b.
- Sarthak Bhagat, Hritwick Banerjee, Zion Tsz Ho Tse, and Hongliang Ren. Deep reinforcement learning for soft, flexible robots: Brief review with impending challenges. *Robotics*, 8(1):4, 2019.
- Aditya Bhatt, Adrian Sieler, Steffen Puhlmann, and Oliver Brock. Surprisingly robust in-hand manipulation: An empirical study. *arXiv preprint arXiv:2201.11503*, 2022.
- Cheng Chi, Zhenjia Xu, Siyuan Feng, Eric Cousineau, Yilun Du, Benjamin Burchfiel, Russ Tedrake, and Shuran Song. Diffusion policy: Visuomotor policy learning via action diffusion. *The International Journal of Robotics Research*, pp. 02783649241273668, 2023.
- Cosimo Della Santina, Antonio Bicchi, and Daniela Rus. On an improved state parametrization for soft robots with piecewise constant curvature and its use in model based control. *IEEE Robotics and Automation Letters*, 5(2):1001–1008, 2020.
- Cosimo Della Santina, Christian Duriez, and Daniela Rus. Model-based control of soft robots: A survey of the state of the art and open challenges. *IEEE Control Systems Magazine*, 43(3):30–65, 2023.
- Charlotte Firth, Kate Dunn, M Hank Haeusler, and Yi Sun. Anthropomorphic soft robotic end-effector for use with collaborative robots in the construction industry. *Automation in Construction*, 138:104218, 2022.

- 594 Zipeng Fu, Tony Z Zhao, and Chelsea Finn. Mobile aloha: Learning bimanual mobile manipulation
595 with low-cost whole-body teleoperation. *arXiv preprint arXiv:2401.02117*, 2024.
596
- 597 Abhishek Gupta, Clemens Eppner, Sergey Levine, and Pieter Abbeel. Learning dexterous manip-
598 ulation for a soft robotic hand from human demonstrations. In *2016 IEEE/RSJ International*
599 *Conference on Intelligent Robots and Systems (IROS)*, pp. 3786–3793. IEEE, 2016.
- 600 Nikolaus Hansen, Sibylle D Müller, and Petros Koumoutsakos. Reducing the time complexity of
601 the derandomized evolution strategy with covariance matrix adaptation (cma-es). *Evolutionary*
602 *computation*, 11(1):1–18, 2003.
603
- 604 Bianca S Homberg, Robert K Katzschmann, Mehmet R Dogar, and Daniela Rus. Robust proprio-
605 ceptive grasping with a soft robot hand. *Autonomous robots*, 43:681–696, 2019.
- 606 Yafei Hu, Quanting Xie, Vidhi Jain, Jonathan Francis, Jay Patrikar, Nikhil Keetha, Seungchan Kim,
607 Yaqi Xie, Tianyi Zhang, Hao-Shu Fang, et al. Toward general-purpose robots via foundation
608 models: A survey and meta-analysis. *arXiv preprint arXiv:2312.08782*, 2023.
609
- 610 Edward Johns. Coarse-to-fine imitation learning: Robot manipulation from a single demonstration.
611 In *2021 IEEE international conference on robotics and automation (ICRA)*, pp. 4613–4619. IEEE,
612 2021.
- 613 Robert K Katzschmann, Cosimo Della Santina, Yasunori Toshimitsu, Antonio Bicchi, and Daniela
614 Rus. Dynamic motion control of multi-segment soft robots using piecewise constant curvature
615 matched with an augmented rigid body model. In *2019 2nd IEEE International Conference on*
616 *Soft Robotics (RoboSoft)*, pp. 454–461. IEEE, 2019.
617
- 618 Fukang Liu, Kavya Puthuveetil, Akhil Padmanabha, Karan Khokar, Zeynep Temel, and Zackory
619 Erickson. Skingrip: An adaptive soft robotic manipulator with capacitive sensing for whole-limb
620 bathing assistance. *arXiv preprint arXiv:2405.02772*, 2024.
- 621 Yang Liu, Seong Hyo Ahn, Uksang Yoo, Alexander R Cohen, and Farshid Alambeigi. Toward ana-
622 lytical modeling and evaluation of curvature-dependent distributed friction force in tendon-driven
623 continuum manipulators. In *2020 IEEE/RSJ International Conference on Intelligent Robots and*
624 *Systems (IROS)*, pp. 8823–8828. IEEE, 2020.
625
- 626 Yang Liu, Uksang Yoo, Seungbeom Ha, S Farokh Atashzar, and Farshid Alambeigi. Influence
627 of antagonistic tensions on distributed friction forces of multisegment tendon-driven continuum
628 manipulators with irregular geometry. *IEEE/ASME Transactions on Mechatronics*, 27(5):2418–
629 2428, 2021.
- 630 Matthew T Mason and J Kenneth Salisbury Jr. Robot hands and the mechanics of manipulation. *The*
631 *MIT Press, Cambridge, MA*, 1985.
632
- 633 Marius Memmel, Jacob Berg, Bingqing Chen, Abhishek Gupta, and Jonathan Francis. Strap: Robot
634 sub-trajectory retrieval for augmented policy learning. In *The Thirteenth International Confer-*
635 *ence on Learning Representations*, 2025. URL [https://openreview.net/forum?id=](https://openreview.net/forum?id=4VHiptx7xe)
636 [4VHiptx7xe](https://openreview.net/forum?id=4VHiptx7xe).
- 637 Amir Pagoli, Frédéric Chapelle, Juan Antonio Corrales, Youcef Mezouar, and Yuri Lapusta. A
638 soft robotic gripper with an active palm and reconfigurable fingers for fully dexterous in-hand
639 manipulation. *IEEE Robotics and Automation Letters*, 6(4):7706–7713, 2021.
640
- 641 Tessa J Pannen, Steffen Puhlmann, and Oliver Brock. A low-cost, easy-to-manufacture, flexible,
642 multi-taxel tactile sensor and its application to in-hand object recognition. In *2022 International*
643 *Conference on Robotics and Automation (ICRA)*, pp. 10939–10944. IEEE, 2022.
- 644 Steffen Puhlmann, Jason Harris, and Oliver Brock. Rbo hand 3: A platform for soft dexterous
645 manipulation. *IEEE Transactions on Robotics*, 38(6):3434–3449, 2022.
646
- 647 Haozhi Qi, Brent Yi, Mike Lambeta, Yi Ma, Roberto Calandra, and Jitendra Malik. From simple to
complex skills: The case of in-hand object reorientation. *arXiv preprint arXiv:2501.05439*, 2025.

- 648 Yuzhe Qin, Wei Yang, Binghao Huang, Karl Van Wyk, Hao Su, Xiaolong Wang, Yu-Wei Chao, and
649 Dieter Fox. Anyteleop: A general vision-based dexterous robot arm-hand teleoperation system.
650 *arXiv preprint arXiv:2307.04577*, 2023.
- 651 Daniela Rus and Michael T Tolley. Design, fabrication and control of soft robots. *Nature*, 521
652 (7553):467–475, 2015.
- 654 Pierre Schegg, Etienne Ménager, Elie Khairallah, Damien Marchal, Jérémie Dequidt, Philippe
655 Preux, and Christian Duriez. Sofagym: An open platform for reinforcement learning based on
656 soft robot simulations. *Soft Robotics*, 10(2):410–430, 2023.
- 657 Adrian Sieler and Oliver Brock. Dexterous soft hands linearize feedback-control for in-hand manip-
658 ulation. In *2023 IEEE/RSJ International Conference on Intelligent Robots and Systems (IROS)*,
659 pp. 8757–8764. IEEE, 2023.
- 661 O Starkova and A Aniskevich. Poisson’s ratio and the incompressibility relation for various strain
662 measures with the example of a silica-filled sbr rubber in uniaxial tension tests. *Polymer Testing*,
663 29(3):310–318, 2010.
- 664 Francesco Stella, Qinghua Guan, Cosimo Della Santina, and Josie Hughes. Piecewise affine curva-
665 ture model: a reduced-order model for soft robot-environment interaction beyond pcc. In *2023*
666 *IEEE International Conference on Soft Robotics (RoboSoft)*, pp. 1–7. IEEE, 2023.
- 668 Javier Tapia, Espen Knoop, Mojmir Mutný, Miguel A Otaduy, and Moritz Bächer. Makesense:
669 Automated sensor design for proprioceptive soft robots. *Soft robotics*, 7(3):332–345, 2020.
- 670 Thomas George Thuruthel, Egidio Falotico, Federico Renda, and Cecilia Laschi. Model-based re-
671 inforcement learning for closed-loop dynamic control of soft robotic manipulators. *IEEE Trans-*
672 *actions on Robotics*, 35(1):124–134, 2018.
- 674 Vincent Wall, Gabriel Zöllner, and Oliver Brock. A method for sensorizing soft actuators and its
675 application to the rbo hand 2. In *2017 IEEE International Conference on Robotics and Automation*
676 *(ICRA)*, pp. 4965–4970. IEEE, 2017.
- 678 Jun Wang, Ying Yuan, Haichuan Che, Haozhi Qi, Yi Ma, Jitendra Malik, and Xiaolong Wang.
679 Lessons from learning to spin “pens”. In *CoRL*, 2024.
- 680 Liangliang Wang, James Lam, Xiaojiao Chen, Jing Li, Runzhi Zhang, Yinyin Su, and Zheng Wang.
681 Soft robot proprioception using unified soft body encoding and recurrent neural network. *Soft*
682 *Robotics*, 10(4):825–837, 2023.
- 684 Ruoyu Wang, Shiheng Wang, Songyu Du, Erdong Xiao, Wenzhen Yuan, and Chen Feng. Real-
685 time soft body 3d proprioception via deep vision-based sensing. *IEEE Robotics and Automation*
686 *Letters*, 5(2):3382–3389, 2020.
- 687 Dehao Wei and Huazhe Xu. A wearable robotic hand for hand-over-hand imitation learning. In
688 *2024 IEEE International Conference on Robotics and Automation (ICRA)*, pp. 18113–18119.
689 IEEE, 2024.
- 691 Abraham Itzhak Weinberg, Alon Shirizly, Osher Azulay, and Avishai Sintov. Survey of learning-
692 based approaches for robotic in-hand manipulation. *Frontiers in Robotics and AI*, 11:1455431,
693 2024.
- 694 JD Westwood et al. Sofa—an open source framework for medical simulation. *Medicine Meets Virtual*
695 *Reality 15: In Vivo, in Vitro, in Silico: Designing the Next in Medicine*, 125:13, 2007.
- 697 Yaoqing Yang, Chen Feng, Yiru Shen, and Dong Tian. Foldingnet: Point cloud auto-encoder via
698 deep grid deformation. In *Proceedings of the IEEE conference on computer vision and pattern*
699 *recognition*, pp. 206–215, 2018.
- 700 Yunchao Yao, Uksang Yoo, Jean Oh, Christopher G Atkeson, and Jeffrey Ichnowski. Soft robotic
701 dynamic in-hand pen spinning. *arXiv preprint arXiv:2411.12734*, 2024.

- 702 Oncay Yasa, Yasunori Toshimitsu, Mike Y Michelis, Lewis S Jones, Miriam Filippi, Thomas Buch-
703 ner, and Robert K Katzschmann. An overview of soft robotics. *Annual Review of Control,*
704 *Robotics, and Autonomous Systems*, 6(1):1–29, 2023.
- 705
706 Uksang Yoo, Yang Liu, Ashish D Deshpande, and Farshid Alamabeigi. Analytical design of a pneu-
707 matic elastomer robot with deterministically adjusted stiffness. *IEEE robotics and automation*
708 *letters*, 6(4):7773–7780, 2021.
- 709 Uksang Yoo, Hanwen Zhao, Alvaro Altamirano, Wenzhen Yuan, and Chen Feng. Toward zero-shot
710 sim-to-real transfer learning for pneumatic soft robot 3d proprioceptive sensing. In *2023 IEEE*
711 *International Conference on Robotics and Automation (ICRA)*, pp. 544–551. IEEE, 2023.
- 712
713 Uksang Yoo, Adam Hung, Jonathan Francis, Jean Oh, and Jeffrey Ichnowski. Ropotter: Toward
714 robotic pottery and deformable object manipulation with structural priors. In *2024 IEEE-RAS*
715 *23rd International Conference on Humanoid Robots (Humanoids)*, pp. 843–850. IEEE, 2024a.
- 716 Uksang Yoo, Ziven Lopez, Jeffrey Ichnowski, and Jean Oh. Poe: Acoustic soft robotic propriocep-
717 tion for omnidirectional end-effectors. *arXiv preprint arXiv:2401.09382*, 2024b.
- 718
719 Uksang Yoo, Nathaniel Dennler, Eliot Xing, Maja Matarić, Stefanos Nikolaidis, Jeffrey Ichnowski,
720 and Jean Oh. Soft and compliant contact-rich hair manipulation and care. *arXiv preprint*
721 *arXiv:2501.02630*, 2025.
- 722 Yanjie Ze, Gu Zhang, Kangning Zhang, Chenyuan Hu, Muhan Wang, and Huazhe Xu. 3d diffusion
723 policy. *arXiv preprint arXiv:2403.03954*, 2024.
- 724
725 Annan Zhang, Tsun-Hsuan Wang, Ryan L Truby, Lillian Chin, and Daniela Rus. Machine learn-
726 ing best practices for soft robot proprioception. In *2023 IEEE/RSJ International Conference on*
727 *Intelligent Robots and Systems (IROS)*, pp. 2564–2571. IEEE, 2023.
- 728
729 Shuai Zhou, Yuanhang Li, Qianqian Wang, and Zhiyang Lyu. Integrated actuation and sensing:
730 Toward intelligent soft robots. *Cyborg and Bionic Systems*, 5:0105, 2024.
- 731
732 Xiaolong Zhou, Xiaoting Chen, and Tianmiao Yang. Soft robotic grippers. *Advanced Intelligent*
733 *Systems*, 5(1):2000198, 2023.
- 734
735
736
737
738
739
740
741
742
743
744
745
746
747
748
749
750
751
752
753
754
755